



# Diagnostic Accuracy of Endocardial-to-Epicardial Myocardial Blood Flow Ratio for the Detection of Significant Coronary Artery Disease With Dynamic Myocardial Perfusion Dual-Source Computed Tomography

Yoshitaka Goto, MD; Kakuya Kitagawa, MD; Mio Uno, MD; Shiro Nakamori, MD;  
Tatsuro Ito, MD; Naoki Nagasawa, PhD; Kaoru Dohi, MD; Hajime Sakuma, MD

**Background:** Previous dynamic stress computed tomography perfusion (CTP) studies used absolute myocardial blood flow (MBF) in mL/100g/min as a threshold to discriminate flow-limiting coronary artery disease (CAD), but absolute MBF can vary because of multiple factors. The aim of this study was to compare the diagnostic performance of absolute MBF and the transmural perfusion ratio (TPR) for the detection of flow-limiting CAD, and to clarify the influence of CT delayed enhancement (CTDE) on the diagnostic performance of CTP.

**Methods and Results:** We retrospectively enrolled 51 patients who underwent dual-source CTP and invasive coronary angiography (ICA). TPR was defined as the endocardial MBF of a specific segment divided by the mean of the epicardial MBF of all segments. Flow-limiting CAD was defined as luminal diameter stenosis >90% on ICA or a lesion with fractional flow reserve  $\leq 0.8$ . Segmental presence and absence of myocardial scar was determined by CTDE. The area under the receiver-operating characteristics curve (AUC) of TPR was significantly greater than that of MBF for the detection of flow-limiting CAD (0.833 vs. 0.711,  $P=0.0273$ ). Myocardial DE was present in 27 of the 51 patients and in 34 of 143 territories. When only territories containing DE were considered, the AUC of TPR decreased to 0.733.

**Conclusions:** TPR calculated from absolute MBF demonstrated higher diagnostic performance for the discrimination of flow-limiting CAD when compared with absolute MBF itself.

**Key Words:** Coronary artery disease; Dual-source computed tomography; Myocardial infarction; Myocardial ischemia; Myocardial perfusion imaging

Coronary computed tomography angiography (CCTA) allows noninvasive assessment of the morphology of coronary artery stenosis and is highly useful for ruling out the presence of obstructive coronary artery disease (CAD).<sup>1,2</sup> However, because obstructive stenosis identified by CCTA is a poor predictor of the presence of myocardial ischemia, a functional test is generally recommended to investigate the hemodynamic significance of the stenotic lesion.<sup>3</sup>

Stress dynamic CT perfusion (CTP) with absolute quantification of myocardial blood flow (MBF) is a new non-invasive technique for the assessment of myocardial ischemia.<sup>4,5</sup> Previous CTP studies used absolute MBF thresholds in mL/100g/min to discriminate flow-limiting CAD,<sup>6–10</sup> but the absolute MBF can vary because of factors other than the degree of coronary artery stenosis.<sup>11–14</sup> Patients with extensive non-obstructive CAD may show

limited response to vasodilator stress, resulting in globally reduced hyperemic MBF.<sup>15</sup> Because the endocardial layer is most susceptible to ischemia,<sup>16,17</sup> the ratio of endocardial MBF and epicardial MBF might be a more useful indicator of flow-limiting CAD.

The purpose of this study was to investigate whether the transmural ratio of absolute MBF can improve the accuracy of CTP when compared with absolute MBF for the detection of flow-limiting CAD, as defined by fractional flow reserve (FFR). We also explored the prevalence of myocardial scar in candidates for CTP and its effect on the diagnostic performance of CTP.

## Methods

### Study Population

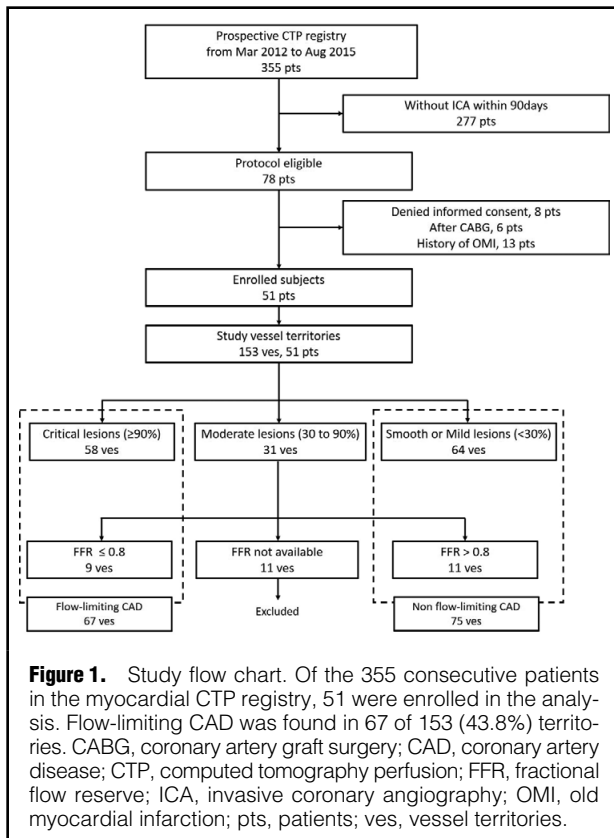
In the comprehensive cardiac CT registry at Mie University

Received December 25, 2016; revised manuscript received March 9, 2017; accepted March 24, 2017; released online April 25, 2017 Time for primary review: 17 days

Department of Radiology (Y.G., K.K., M.U., T.I., N.N., H.S.), Department of Cardiology (S.N., K.D.), Mie University Hospital, Tsu, Japan

Mailing address: Kakuya Kitagawa, MD, Department of Radiology, Mie University Hospital, 2-174 Edobashi, Tsu 514-8507, Japan. E-mail: kakuya@clin.medic.mie-u.ac.jp

ISSN-1346-9843 All rights are reserved to the Japanese Circulation Society. For permissions, please e-mail: cj@j-circ.or.jp



Hospital, we identified a total of 355 patients who had undergone a comprehensive cardiac CT study by dual-source CT (SOMATOM Definition Flash; Siemens Healthcare, Forchheim, Germany) consisting of adenosine-stress dynamic CTP, rest CCTA and CT delayed enhancement [CTDE]) between March 2012 and August 2015. The comprehensive CT protocol was indicated for patients between 45 and 85 years of age who were referred for CCTA with known or suspected CAD. Patients with impaired renal function (estimated glomerular filtration rate  $<30$  mL/min/1.73 m<sup>2</sup> body surface area), known allergy to iodinated contrast agent, or contraindication against adenosine were to be excluded, but none of the identified patients met any of these exclusion criteria. For this study, we retrospectively identified 78 patients who underwent invasive coronary angiography (ICA) within 90 days of the CT examination. After exclusion of patients who did not provide informed consent (n=8), patients who underwent coronary arterial bypass graft surgery (n=6), and patients with a history of myocardial infarction (n=13), 51 patients comprised the final study population (**Figure 1**). No patient experienced revascularization therapy or change in medications between CT and ICA. This study was approved by the institutional review board, and written informed consent for participation in the study was given by each patient.

### CT Data Acquisition and Reconstruction

During a 3-min administration of adenosine (Adenoscan; Daiichi-Sankyo, Tokyo, Japan) at 0.14 mg/kg/min,<sup>18,19</sup> dynamic myocardial CTP was initiated with injection of 40 mL of iopamidol with an iodine concentration of 370 mgI/mL at a flow rate of 5 mL/s. Dynamic datasets

were acquired for 30 s using ECG-triggered axial scan mode with alternating table position “shuttle modes scan” with a Z-axis coverage of 73 mm.<sup>20</sup> On completion of the imaging, adenosine administration was discontinued. ECG, blood pressure, and arterial oxygen saturation were monitored throughout the procedure.

Standard prospective CCTA at rest was performed after stress dynamic CTP using the following scan parameters: 2×100 kV tube voltage or 80 kV and 0.28-s gantry rotation time, with injection of 0.84 mL/kg of iopamidol in 12 s. Tube current was determined using the angular-modulation technique.<sup>21,22</sup>

Myocardial CTDE images were acquired 7 min after CCTA without additional contrast administration and were reconstructed with a method described previously.<sup>23</sup> Tube voltage and tube current setting were 80 kV and 370 mA, respectively.

### CT Perfusion and CTDE Data Evaluation

The dynamic CTP data were analyzed with commercially available perfusion software (Syngo VPCT body, Siemens Healthcare). As has been previously described,<sup>24</sup> MBF was estimated using a dedicated parametric deconvolution technique based on a 2-compartment model of the intravascular and extravascular spaces to fit the time attenuation curves. The algorithm then generated a MBF map with 3-mm thickness and 1-mm increments by applying the maximum slope approach onto the model curve that was fit for every voxel. The MBF map was analyzed using in-house software written on MATLAB (MathWorks, Natick, MA, USA) by 2 independent observers (**Figure S1**). Endocardial and epicardial borders of the left ventricular myocardium were manually traced on short-axis slices and then the subendocardial MBF and subepicardial MBF in each of the 16 segments, excluding the apical segment of the American College of Cardiology/American Heart Association 17-segment model, were calculated automatically.

To estimate the transmural distribution of perfusion abnormalities, the transmural perfusion ratio (TPR) was calculated as the subendocardial MBF of a specific segment divided by the mean subepicardial MBF of all 16 segments.<sup>25</sup> Minimum MBF of subendocardial segments and minimum TPR were used for analysis.

By using multiplanar image stacks aligned with the short-axis and long-axis of the left ventricle (5-mm thickness, 5-mm increment, window width/window level=200/100), CTDE images were analyzed visually to determine the presence and absence of hyperenhancement suggestive of infarct scar within each segment of the 16 segments by the consensus of 2 observers who were unaware of the CTP, CCTA and ICA results.<sup>26,27</sup>

CCTA images were reviewed to confirm the correct assignment of the myocardial segment to the coronary artery territories using previously described methods.<sup>28</sup> The myocardial segment was reassigned in 7 of the 51 patients according to coronary artery anatomy.

### ICA and FFR

ICA images were analyzed visually on multiple projections by the consensus of 2 experienced cardiologists who were unaware of the CT results. Segments with a diameter  $<1.5$  mm were excluded from analysis. Critical lesions ( $\geq 90\%$  diameter narrowing) were classified as hemodynamically significant stenosis, while mild lesions ( $<30\%$  diameter nar-

**Table 1. Patients' Baseline Characteristics and Main Findings on Invasive Coronary Angiography**

Characteristic	Total (n=51)
Men/women	40/11 (78.4/21.6)
Age (years)	68.5±7.8
Body mass index (kg/m <sup>2</sup> )	23.5±3.6
<b>Coronary risk factors</b>	
Hypertension	35 (83.3)
Diabetes mellitus	25 (49.1)
Dyslipidemia	38 (74.5)
Current smoker	10 (19.6)
Family history of CAD	10 (19.6)
<b>Right dominant coronary system</b>	49 (96.1)
<b>Prior stent implantation</b>	7 (13.7)
<b>Hemodynamically significant stenosis coronary lesion</b>	
1-vessel disease	19 (37.3)
2-vessel disease	12 (23.5)
3-vessel disease	8 (15.7)

Values are mean±SD, or frequency (percentages), unless otherwise specified. CAD, coronary artery disease.

rowing) were classified as non-significant.<sup>29</sup> The hemodynamic significance of moderate lesions (30–90% diameter narrowing) was determined by FFR.

FFR was measured using a sensor-tipped 0.014-inch guidewire (Pressure Wire Certus, Radi Medical Systems, Uppsala, Sweden). The pressure sensor was positioned just distal to the lesion, and maximal myocardial hyperemia was induced by a continuous intravenous infusion of adenosine (0.14 mg/kg/min for a minimum of 2 min).<sup>30,31</sup> The FFR was calculated as the ratio of mean distal pressure measured by the pressure wire divided by the mean proximal pressure measured by the guiding catheter. FFR ≤0.8 was chosen to define hemodynamically significant stenosis in the lesion and its supplied territory.<sup>32</sup>

**Table 2. Radiation Dose and Vital Signs in CT Examination**

Parameter	
<b>Radiation exposure (mSv)</b>	
Comprehensive CT study	11.3±2.3
CTP	5.3±2.1
CCTA	2.6±1.6
CTDE	1.8±0.1
<b>Heart rate (beats/min)</b>	
Baseline	62.5±10.6
During adenosine stress	70.3±12.4
<b>Systolic BP (mmHg)</b>	
Baseline	141.3±24.5
During adenosine stress	124.4±22.1
<b>Diastolic BP (mmHg)</b>	
Baseline	71.8±12.3
During adenosine stress	64.4±14.1

BP, blood pressure; CTP, computed tomography perfusion; CCTA, coronary computed tomography angiography; CTDE, computed tomography delayed enhancement.

### Statistical Analysis

Continuous variables are presented as mean±standard deviation if normally distributed. Categorical variables are displayed as frequency (percentage). Distribution of the continuous variables was assessed using the Shapiro-Wilk test. Differences within groups were compared using the paired Student t-test for normally distributed variables, or the Mann-Whitney signed rank test for independent samples and non-parametric variables. Sensitivity, specificity, positive predictive value (PPV), negative predictive value (NPV), and 95% confidence intervals (CI) were calculated to predict the ability of each index to identify hemodynamically significant stenoses on a per-vessel (left anterior descending coronary artery [LAD], left circumflex coro-

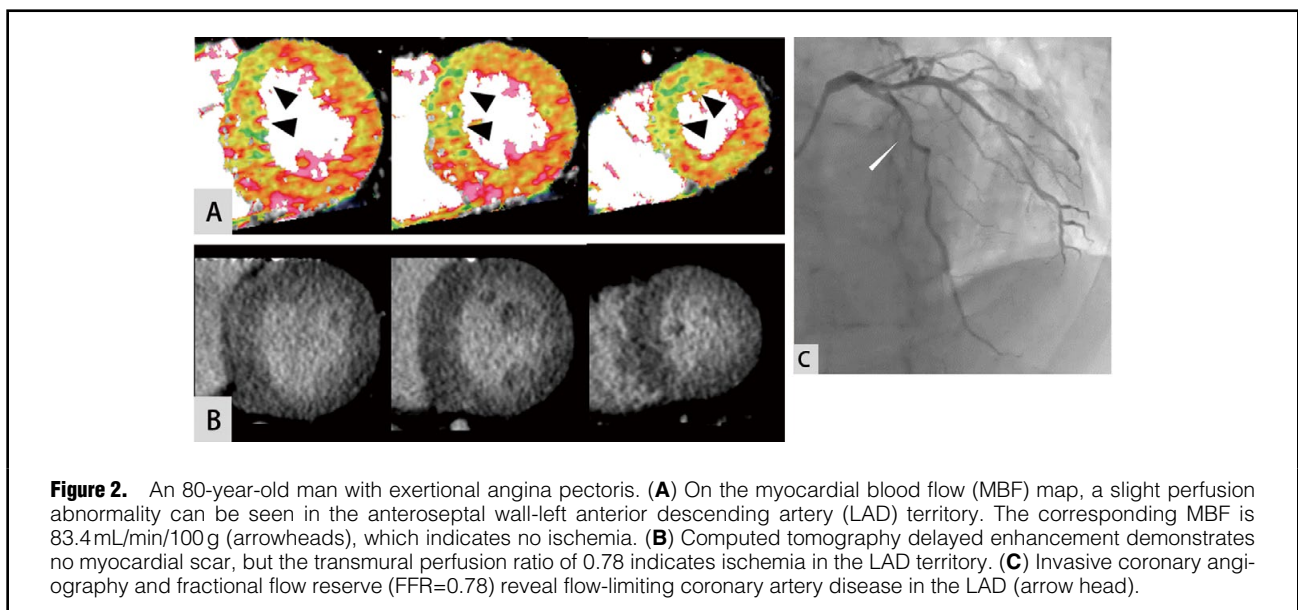


**Figure 2.** An 80-year-old man with exertional angina pectoris. (A) On the myocardial blood flow (MBF) map, a slight perfusion abnormality can be seen in the anteroseptal wall-left anterior descending artery (LAD) territory. The corresponding MBF is 83.4 mL/min/100 g (arrowheads), which indicates no ischemia. (B) Computed tomography delayed enhancement demonstrates no myocardial scar, but the transmural perfusion ratio of 0.78 indicates ischemia in the LAD territory. (C) Invasive coronary angiography and fractional flow reserve (FFR=0.78) reveal flow-limiting coronary artery disease in the LAD (arrow head).

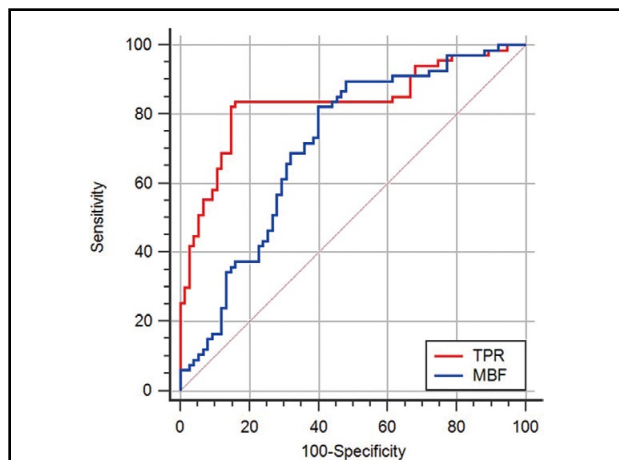


**Figure 3.** Receiver-operating characteristics curves of endomyocardial blood flow (MBF) and transmural perfusion ratio (TPR) for detection of flow-limiting coronary artery disease. TPR (AUC=0.833) shows significantly higher diagnostic performance than MBF (AUC=0.711) ( $P=0.0273$ ). AUC, area under the receiver-operating characteristic curve.

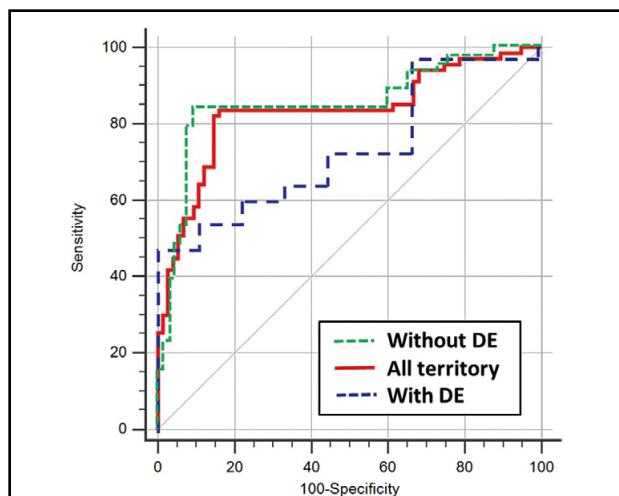


**Figure 4.** Influence of the presence and absence of delayed enhancement (DE) on receiver-operating characteristics curves of TPR detecting flow-limiting coronary artery disease. The AUC of TPR for the detection of flow-limiting coronary stenosis is 0.733 (95% CI, 0.554–0.870), when only territories containing DE were considered. Exclusion of territories containing DE improved the AUC of TPR from 0.833 to 0.838 (95% CI, 0.756 to 0.901), but the effect was not statistically significant comparing with all territories ( $P=0.930$ ). CI, confidence interval. Other abbreviations as in Figure 3.

nary artery [LCX], and right coronary artery [RCA]) basis and a per-patient basis. Receiver-operating characteristic (ROC) curve analysis was undertaken to evaluate the discriminatory ability of MBF and TPR for hemodynamically significant stenosis on a per-vessel basis and a per-patient basis. The areas under the ROC curves (AUCs) derived from the same cases were compared by using the approach of DeLong et al<sup>33</sup> and the different cases were compared using the approach of Hanley and McNeil.<sup>34</sup>

Optimal cutoff values for MBF and TPR were calculated as the thresholds maximizing the Youden index  $J$ , where  $J = \text{sensitivity} + \text{specificity} - 1$ . Sensitivity and specificity were calculated for the cutoff values. Intraobserver and interobserver variabilities were compared using the intraclass correlation coefficient for absolute agreement. A two-sided value of  $P < 0.05$  was considered to represent statistical significance. All analyses were performed with the MedCalc (version 13.2.2 MedCalc Software, Mariakerke, Belgium).

## Results

### Baseline Characteristics

Patient characteristics are summarized in **Table 1**. The comprehensive CT protocol and ICA were successfully done without major adverse events. No patients and no vessel territories were excluded because of CT image quality. A total of 7 patients (13.7%) and 13 vessels (8.5%) had prior stent implantation for stable angina pectoris. There was no patient with a left ventricular wall thickness  $> 13$  mm on echocardiography.

### ICA and FFR Findings

On ICA, 46 patients (90.2%) had  $> 30\%$  stenosis in at least 1 coronary artery. On a territory basis, 58 territories (37.9%) had critical lesions, 31 territories (20.3%) had moderate lesions, and 64 territories (41.8%) had angiographically mild lesions. Of the 31 territories with moderate lesion, FFR results were not available for 11 territories (11/31, 35.5%), which were excluded from the analysis. The remaining 20 territories were successfully interrogated, demonstrating a FFR  $\leq 0.80$  in 9 territories (9/20, 45.0%). Thus, data from 142 territories (46 LAD, 47 LCX and 49 RCA) were available for comparison and were included in the analysis. A total of 67 territories (67/142, 47.2%, [29 LAD, 22 LCX and 16 RCA]) in 39 patients (39/51, 76.5%) were identified as territories with flow-limiting CAD (**Figure 1**).

### CT and MBF Results

**Table 2** demonstrates the CT scan parameters. The mean heart rate significantly increased from  $62.5 \pm 10.6$  beats/min at baseline to  $70.3 \pm 12.4$  beats/min with adenosine administration ( $P < 0.0001$ ). The mean systolic blood pressure significantly decreased from  $141.3 \pm 24.5$  mmHg at baseline to  $124.4 \pm 22.1$  mmHg with adenosine administration, while the diastolic blood pressure significantly decreased from  $71.8 \pm 12.3$  mmHg to  $64.4 \pm 14.1$  mmHg ( $P < 0.0001$  and  $P < 0.0001$ ). The mean MBF of all myocardial segments, all subepicardial myocardium, and all subendocardial myocardium on dynamic stress perfusion CT was  $98.1 \pm 34.6$  mL/100 mL/min (range, 41.2–173.6 mL/100 mL/min),  $99.8 \pm 34.6$  mL/100 mL/min (range, 41.1–175.4 mL/100 mL/min) and  $97.1 \pm 35.0$  mL/100 mL/min (range, 39.1–172.1 mL/100 mL/min), respectively. Representative images are provided in **Figure 2**.

### Diagnostic Performance of MBF Indices

At the territory level, both MBF and TPR were significantly different between those with flow-limiting CAD and those without ( $73.5 \pm 26.5$  mL/100 g/min vs.  $98.6 \pm 36.0$  mL/100 g/min,  $P < 0.0001$ , and  $0.811 \pm 0.136$  vs.  $0.966 \pm 0.094$ ,  $P < 0.0001$ , respectively). On ROC curve analysis, MBF had an AUC of 0.711 (95% CI, 0.629–0.784). TPR had a significantly greater AUC of 0.833 (95%

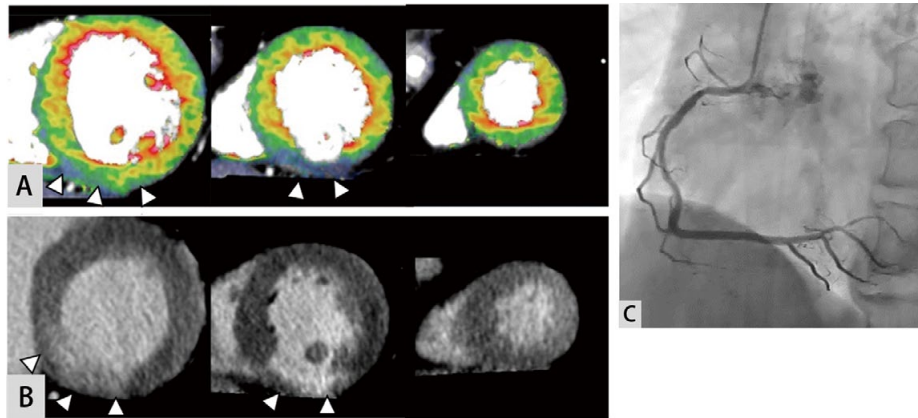


**Figure 5.** A 57-year-old man with a stent in the right coronary artery (RCA). **(A)** Myocardial blood flow is 54.6 mL/min/100 g in the RCA (arrowheads). The corresponding transmural perfusion ratio is 0.78. Both results indicate myocardial ischemia. Invasive coronary angiography **(C)** shows no in-stent restenosis and no other stenosis in the RCA, so the false-positive result of computed tomography perfusion can be explained by the presence of myocardial scar, which is clearly revealed by computed tomography delayed enhancement (arrowheads) **(B)**.

CI, 0.761–0.890,  $P=0.0273$ ) (**Figure 3**). With a cutoff value of 0.899, TPR showed a sensitivity, specificity, PPV, NPV and accuracy of 83.6% (56/67), 84.0% (63/75), 82.4% (56/68), 85.9% (63/74) and 83.8% (119/142), respectively. With a cutoff value of 89.0, MBF showed a sensitivity, specificity, PPV, NPV and accuracy of 82.1% (55/67), 60.0% (45/75), 64.7% (55/85), 78.9% (45/64) and 70.4% (100/142), respectively.

At the patient level, on ROC curve analysis, MBF had an AUC of 0.703 (95% CI, 0.559–0.823). Although the AUC of TPR (0.840; 95% CI, 0.710–0.927) was greater than that of MBF, the difference was not statistically significant ( $P=0.307$ ). With a cutoff value of 0.899, TPR showed a sensitivity, specificity, PPV, NPV and accuracy of 89.4% (35/39), 66.7% (8/12), 89.7% (35/39), 66.7% (8/12) and 84.3% (35/51), respectively. With a cutoff value of 90.2, MBF showed a sensitivity, specificity, PPV, NPV and accuracy of 79.5% (31/39), 66.7% (8/12), 88.6% (31/35), 50.0% (8/16) and 76.5% (39/51), respectively.

Intraobserver and interobserver intraclass correlation coefficients of vessel territory level were, respectively, 0.934 (95% CI, 0.902–0.956) and 0.913 (95% CI, 0.873–0.940) for MBF and 0.917 (95% CI, 0.879–0.943) and 0.835 (95% CI, 0.758–0.888) for TPR.

#### Prevalence of Myocardial DE and Its Effect on Diagnostic Performance of CTP

Myocardial DE was present in 21 of 51 patients (41.2%) and in 34 of 143 territories (23.8%). All myocardial DE involved the subendocardium in a coronary distribution. Among the 7 patients who with prior stent implantation, 6 (85.7%) had a DE lesion. Prevalence of DE in stent-implanted vessels was also high (6/13 [46.2%]). Of the 6 vessel territories with DE, only one was flow-limiting despite reduced TPR. Even in subjects without stent implantation, prevalence of DE was relatively high (28/130 territories [21.5%] in 15/44 patients [34.1%]) in the current study population who had no clinical history of myocardial infarction. Of the 28 vessel territories with DE, 24 were supplied by flow-limited vessels.

When only those containing DE were considered, the AUC of TPR for detecting flow-limiting coronary stenosis was 0.733 (95% CI, 0.554–0.870), with a sensitivity, specificity, PPV and NPV of 88.0% (22/25), 33.3% (3/9), 78.5% (22/28) and 50.0% (3/6), respectively. Exclusion of territories containing DE improved the AUC of TPR from 0.833 to 0.838 (95% CI, 0.756–0.901), but the effect was not statistically significant ( $P=0.930$ ) (**Figure 4**).

#### Discussion

The major findings of this study were: (1) TPR calculated from absolute MBF yielded higher diagnostic performance for discriminating flow-limiting CAD when compared with absolute MBF itself, and (2) there was a high prevalence of myocardial scar detected by CTDE in patients who underwent comprehensive cardiac CT and subsequent ICA after excluding subjects with a history of myocardial infarction.

There are a number of pathophysiological and methodological factors that can affect absolute MBF in the vasodilator-induced hyperemic state,<sup>11</sup> which may explain the wide range of optimal MBF cutoff values to detect ischemia among previous studies.<sup>6–10</sup> Because it is well established that the endocardial layer is more susceptible to ischemia and that perfusion of epicardial layers is relatively spared, even in the presence of severe coronary stenosis, one can assume that the relative flow index focussing on the difference between the endocardium and epicardium accurately reflects stenosis severity better than absolute thresholds.<sup>17</sup> Indeed, the TPR of absolute MBF, a ratio of endocardial MBF and epicardial MBF, improved the accuracy of stress dynamic CT for the detection of flow-limiting CAD in our study.

George et al<sup>25</sup> were the first to describe the utility of transmural differences in the attenuation CT density in the subendocardial and subepicardial layers of the left ventricle during adenosine stress. They used TPR derived from static CTP (assessment of myocardial perfusion obtained from a single data sample) and demonstrated that TPR can predict myocardial perfusion abnormalities in the setting

of obstructive atherosclerosis in comparison with combined quantitative coronary angiography and single-photon emission computed tomography. However, the CT density of the myocardium on static CT perfusion imaging is highly dependent on the contrast material bolus profile as well as on data acquisition timing.<sup>35</sup> A previous cardiac magnetic resonance study analyzed the transmural gradient in myocardial contrast uptake as signal intensity using dynamic magnetic resonance perfusion.<sup>36</sup> That study indicated that the transmural gradient of the signal intensity in the left ventricular myocardium can be affected by the timing of contrast material administration and that it varies over time. The same might be equally true with regard to the transmural differences in the attenuation CT density, while the TPR of the absolute MBF might be less affected by acquisition timing issues. Superior diagnostic performance of the CT-derived relative MBF value has been demonstrated for the detection of significant coronary artery stenosis when compared with absolute MBF values.<sup>37,38</sup> Kono et al demonstrated that the AUC of the relative MBF value was significantly greater than that of the absolute MBF value (0.87 and 0.75, respectively). Their AUCs were comparable with our current results. However, their relative MBF values were not TPR, rather, they were ratios of the absolute MBF divided by the highest remote MBF value, which may be strongly affected by the selection of regions of interest.

Analysis of the prevalence of myocardial DE in candidates for CTP is a unique feature of the current study. We found a high prevalence of myocardial DE of 41.2% in all subjects and of 34.1% in subjects without stent implantation. In this study, all DE lesions involved the subendocardium in a coronary distribution, which is typical of myocardial infarction and 73% of those myocardial DE were associated with a flow-limited epicardial coronary artery.<sup>26,27</sup> We anticipated a deterioration in the accuracy of CTP as a result of the high prevalence of myocardial DE because myocardial scar or infarction is likely to show reduced MBF regardless of the presence or absence of flow-limiting CAD. In reality, myocardial DE had only a small effect on the diagnostic performance of CTP in the territories without previous stent implantation because the presence of myocardial DE is almost always associated with both reduced TPR and significant stenosis in the epicardial coronary artery.

The presence of myocardial DE is probably more clinically problematic in patients with prior stent implantation, because the myocardial DE in per-stent-implanted vessels was as high as 46% in our study and because all of these DE lesions demonstrated reduced MBF regardless of the presence or absence of in-stent restenosis, as exemplified in **Figure 5**. Our finding explains the extremely low PPV of CTP for the detection of in-stent restenosis as reported by Rief et al.<sup>39</sup> For CTP to be truly useful in the evaluation of in-stent restenosis, differentiation between ischemia and infarction is necessary. The comprehensive CT study protocol in this study can provide discrimination of myocardial ischemia and infarction. Further study is needed to evaluate the utility of comprehensive CT study for diagnosing in-stent restenosis.

### Study Limitations

Our study had several. First, it was a single-center study with a small sample size. Second, patients with an intermediate or high probability of CAD were evaluated, so selec-

tion bias could have had some effect on the results. Third, not all vessels were interrogated with FFR. FFR evaluation was not performed in vessels with <30% diameter narrowing, as angiographically normal, or in >90% diameter narrowing as significant stenosis. Although that was in agreement with generally accepted clinical standards, the effect of coronary collateral circulation on myocardial ischemia was not considered.<sup>40</sup> Fourth, combining CTCA with CTP will increase the ionizing radiation dose as well as the contrast medium volume. Fifth, CTDE was performed for the detection of myocardial scar, but late gadolinium enhancement cardiac magnetic resonance, which is widely accepted as the standard noninvasive imaging technique for detecting myocardial scar, was not performed.

### Conclusions

TPR obtained from quantitative stress dynamic dual-source CT perfusion demonstrated higher diagnostic performance for discriminating flow-limiting CAD when compared with absolute MBF. There was a high prevalence of myocardial DE detected by CTDE in patients who had undergone comprehensive cardiac CT and subsequent ICA but had no history of myocardial infarction.

### Conflict of Interest Statement

Hajime Sakuma received a research grant from Siemens Healthcare K.K. and Bayer Yakuhin, Ltd.

### Name of Grant

The authors state that this work has not received any funding.

### References

1. Miller JM, Rochitte CE, Dewey M, Arbab-Zadeh A, Niinuma H, Gottlieb I, et al. Diagnostic performance of coronary angiography by 64-row CT. *N Engl J Med* 2008; **359**: 2324–2336.
2. Budoff MJ, Dowe D, Jollis JG, Gitter M, Sutherland J, Halamert E, et al. Diagnostic performance of 64-multidetector row coronary computed tomographic angiography for evaluation of coronary artery stenosis in individuals without known coronary artery disease: Results from the prospective multicenter ACCURACY (Assessment by Coronary Computed Tomographic Angiography of Individuals Undergoing Invasive Coronary Angiography) trial. *J Am Coll Cardiol* 2008; **52**: 1724–1732.
3. Meijboom WB, Van Mieghem CA, van Pelt N, Weustink A, Pugliese F, Mollet NR, et al. Comprehensive assessment of coronary artery stenoses: Computed tomography coronary angiography versus conventional coronary angiography and correlation with fractional flow reserve in patients with stable angina. *J Am Coll Cardiol* 2008; **52**: 636–643.
4. Bamberg F, Klotz E, Flohr T, Becker A, Becker CR, Schmidt B, et al. Dynamic myocardial stress perfusion imaging using fast dual-source CT with alternating table positions: Initial experience. *Eur Radiol* 2010; **20**: 1168–1173.
5. Dwivedi G, Dowsley TF, Chow BJ. Assessment of cardiac computed tomography-myocardial perfusion imaging: Promise and challenges. *Circ J* 2012; **76**: 544–552.
6. Rossi A, Dharampal A, Wragg A, Davies LC, van Geuns RJ, Anagnostopoulos C, et al. Diagnostic performance of hyperaemic myocardial blood flow index obtained by dynamic computed tomography: Does it predict functionally significant coronary lesions? *Eur Heart J Cardiovasc Imaging* 2014; **15**: 85–94.
7. Bamberg F, Marcus RP, Becker A, Hildebrandt K, Bauner K, Schwarz F, et al. Dynamic myocardial CT perfusion imaging for evaluation of myocardial ischemia as determined by MR imaging. *JACC Cardiovasc Imaging* 2014; **7**: 267–277.
8. Greif M, von Ziegler F, Bamberg F, Tittus J, Schwarz F, D'Anastasi M, et al. CT stress perfusion imaging for detection of haemodynamically relevant coronary stenosis as defined by FFR. *Heart* 2013; **99**: 1004–1011.
9. Ho KT, Chua KC, Klotz E, Panknin C. Stress and rest dynamic myocardial perfusion imaging by evaluation of complete time-

- attenuation curves with dual-source CT. *JACC Cardiovasc Imaging* 2010; **3**: 811–820.
10. Wang Y, Qin L, Shi X, Zeng Y, Jing H, Schoepf UJ, et al. Adenosine-stress dynamic myocardial perfusion imaging with second-generation dual-source CT: Comparison with conventional catheter coronary angiography and SPECT nuclear myocardial perfusion imaging. *Am J Roentgenol* 2012; **198**: 521–529.
  11. Gould KL, Kirkeeide RL, Buchi M. Coronary flow reserve as a physiologic measure of stenosis severity. *J Am Coll Cardiol* 1990; **15**: 459–474.
  12. Chareonthaitawee P, Kaufmann PA, Rimoldi O, Camici PG. Heterogeneity of resting and hyperemic myocardial blood flow in healthy humans. *Cardiovasc Res* 2001; **50**: 151–161.
  13. Liga R, Rovai D, Sampietro T, Vecoli C, Todiere G, Caselli C, et al. Insulin resistance is a major determinant of myocardial blood flow impairment in anginal patients. *Eur J Nucl Med Mol Imaging* 2013; **40**: 1905–1913.
  14. Danad I, Rajmakers PG, Appelman YE, Harms HJ, de Haan S, van den Oever ML, et al. Coronary risk factors and myocardial blood flow in patients evaluated for coronary artery disease: A quantitative [<sup>15</sup>O]H<sub>2</sub>O PET/CT study. *Eur J Nucl Med Mol Imaging* 2012; **39**: 102–112.
  15. Kaufmann PA, Camici PG. Myocardial blood flow measurement by PET: Technical aspects and clinical applications. *J Nucl Med* 2005; **46**: 75–88.
  16. Reimer KA, Lowe JE, Rasmussen MM, Jennings RB. The wave-front phenomenon of ischemic cell death. I: Myocardial infarct size vs duration of coronary occlusion in dogs. *Circulation* 1977; **56**: 786–794.
  17. Mordini FE, Haddad T, Hsu LY, Kellman P, Lowrey TB, Aletras AH, et al. Diagnostic accuracy of stress perfusion CMR in comparison with quantitative coronary angiography: Fully quantitative, semiquantitative, and qualitative assessment. *JACC Cardiovasc Imaging* 2014; **7**: 14–22.
  18. Kramer CM, Barkhausen J, Flamm SD, Kim RJ, Nagel E; Society for Cardiovascular Magnetic Resonance Board of Trustees Task Force on Standardized Protocols. Standardized cardiovascular magnetic resonance (CMR) protocols 2013 update. *J Cardiovasc Magn Reson* 2013; **15**: 91.
  19. Henzlova MJ, Duvall WL, Einstein AJ, Travin MI, Verberne HJ. ASNC imaging guidelines for SPECT nuclear cardiology procedures: Stress, protocols, and tracers. *J Nucl Cardiol* 2016; **23**: 606–639.
  20. Bamberg F, Becker A, Schwarz F, Marcus RP, Greif M, von Ziegler F, et al. Detection of hemodynamically significant coronary artery stenosis: Incremental diagnostic value of dynamic CT-based myocardial perfusion imaging. *Radiology* 2011; **260**: 689–698.
  21. Gress H, Nomayr A, Wolf H, Baum U, Lell M, Bowing B, et al. Dose reduction in CT examination of children by an attenuation-based on-line modulation of tube current (CARE Dose). *Eur Radiol* 2002; **12**: 1571–1576.
  22. Fujita M, Kitagawa K, Ito T, Shiraishi Y, Kurobe Y, Nagata M, et al. Dose reduction in dynamic CT stress myocardial perfusion imaging: Comparison of 80-kV/370-mAs and 100-kV/300-mAs protocols. *Eur Radiol* 2014; **24**: 748–755.
  23. Kurobe Y, Kitagawa K, Ito T, Kurita Y, Shiraishi Y, Nakamori S, et al. Myocardial delayed enhancement with dual-source CT: Advantages of targeted spatial frequency filtration and image averaging over half-scan reconstruction. *J Cardiovasc Comput Tomogr* 2014; **8**: 289–298.
  24. Mahnken AH, Klotz E, Pietsch H, Schmidt B, Allmendinger T, Haberland U, et al. Quantitative whole heart stress perfusion CT imaging as noninvasive assessment of hemodynamics in coronary artery stenosis: Preliminary animal experience. *Invest Radiol* 2010; **45**: 298–305.
  25. George RT, Arbab-Zadeh A, Miller JM, Kitagawa K, Chang HJ, Bluemke DA, et al. Adenosine stress 64- and 256-row detector computed tomography angiography and perfusion imaging: A pilot study evaluating the transmural extent of perfusion abnormalities to predict atherosclerosis causing myocardial ischemia. *Circ Cardiovasc Imaging* 2009; **2**: 174–182.
  26. Kim RJ, Albert TS, Wible JH, Elliott MD, Allen JC, Lee JC, et al. Performance of delayed-enhancement magnetic resonance imaging with gadoversetamide contrast for the detection and assessment of myocardial infarction: An international, multi-center, double-blinded, randomized trial. *Circulation* 2008; **117**: 629–637.
  27. Schelbert EB, Cao JJ, Sigurdsson S, Aspelund T, Kellman P, Aletras AH, et al. Prevalence and prognosis of unrecognized myocardial infarction determined by cardiac magnetic resonance in older adults. *JAMA* 2012; **308**: 890–896.
  28. Ko BS, Cameron JD, Meredith IT, Leung M, Antonis PR, Nasis A, et al. Computed tomography stress myocardial perfusion imaging in patients considered for revascularization: A comparison with fractional flow reserve. *Eur Heart J* 2012; **33**: 67–77.
  29. Tonino PA, Fearon WF, De Bruyne B, Oldroyd KG, Leeser MA, Ver Lee PN, et al. Angiographic versus functional severity of coronary artery stenoses in the FAME study fractional flow reserve versus angiography in multivessel evaluation. *J Am Coll Cardiol* 2010; **55**: 2816–2821.
  30. Montalescot G, Sechtem U, Achenbach S, Andreotti F, Arden C, Budaj A, et al. 2013 ESC guidelines on the management of stable coronary artery disease: The Task Force on the management of stable coronary artery disease of the European Society of Cardiology. *Eur Heart J* 2013; **34**: 2949–3003.
  31. Levine GN, Bates ER, Blankenship JC, Bailey SR, Bittl JA, Cercek B, et al. 2011 ACCF/AHA/SCAI Guideline for Percutaneous Coronary Intervention: A report of the American College of Cardiology Foundation/American Heart Association Task Force on Practice Guidelines and the Society for Cardiovascular Angiography and Interventions. *J Am Coll Cardiol* 2011; **58**: e44–e122.
  32. Tonino PA, De Bruyne B, Pijls NH, Siebert U, Ikeno F, van't Veer M, et al. Fractional flow reserve versus angiography for guiding percutaneous coronary intervention. *N Engl J Med* 2009; **360**: 213–224.
  33. DeLong ER, DeLong DM, Clarke-Pearson DL. Comparing the areas under two or more correlated receiver operating characteristic curves: A nonparametric approach. *Biometrics* 1988; **44**: 837–845.
  34. Hanley JA, McNeil BJ. The meaning and use of the area under a receiver operating characteristic (ROC) curve. *Radiology* 1982; **143**: 29–36.
  35. Tanabe Y, Kido T, Kurata A, Uetani T, Fukuyama N, Yokoi T, et al. Optimal scan time for single-phase myocardial computed tomography perfusion to detect myocardial ischemia- derivation cohort from dynamic myocardial computed tomography perfusion. *Circ J* 2016; **80**: 2506–2512.
  36. Hautvast GL, Chiribiri A, Lockie T, Breeuwer M, Nagel E, Plein S. Quantitative analysis of transmural gradients in myocardial perfusion magnetic resonance images. *Magn Reson Med* 2011; **66**: 1477–1487.
  37. Wichmann JL, Meinel FG, Schoepf UJ, Lo GG, Choe YH, Wang Y, et al. Absolute versus relative myocardial blood flow by dynamic CT myocardial perfusion imaging in patients with anatomic coronary artery disease. *Am J Roentgenol* 2015; **205**: W67–W72.
  38. Kono AK, Coenen A, Lubbers M, Kurata A, Rossi A, Dharampal A, et al. Relative myocardial blood flow by dynamic computed tomographic perfusion imaging predicts hemodynamic significance of coronary stenosis better than absolute blood flow. *Invest Radiol* 2014; **49**: 801–807.
  39. Rief M, Zimmermann E, Stenzel F, Martus P, Stangl K, Greupner J, et al. Computed tomography angiography and myocardial computed tomography perfusion in patients with coronary stents: Prospective intraindividual comparison with conventional coronary angiography. *J Am Coll Cardiol* 2013; **62**: 1476–1485.
  40. Matsuo H, Watanabe S, Kadosaki T, Yamaki T, Tanaka S, Miyata S, et al. Validation of collateral fractional flow reserve by myocardial perfusion imaging. *Circulation* 2002; **105**: 1060–1065.

### Supplementary Files

#### Supplementary File 1

**Figure S1.** MBF map analysis using in-house software written in MATLAB.

Please find supplementary file(s);  
<http://dx.doi.org/10.1253/circj.CJ-16-1319>